Integrity-Oriented Content Transmission in Highway Vehicular Ad Hoc Networks

Tom H. Luan*, Xuemin (Sherman) Shen*, Fan Bai†
* Department of Electrical and Computer Engineering, University of Waterloo, Waterloo, ON, Canada, N2L 3G1
† Electrical and Controls Integration Lab, General Motors Global R&D, Warren, MI 48105, USA
Email: {hluan, xshen}@bbcr.uwaterloo.ca, fan.bai@gm.com

***Abstract*—The effective inter-vehicle transmission of content files, *e.g.*, images, music and video clips, is the basis of media communications in vehicular networks, such as social communications and video sharing. However, due to the presence of diverse node velocities, severe channel fadings and intensive mutual interferences among vehicles, the inter-vehicle or vehicle-to-vehicle (V2V) communications tend to be transient and highly dynamic. Content transmissions among vehicles over the volatile and spotty V2V channels are thus susceptible to frequent interruptions and failures, resulting in many fragment content transmissions which are unable to finish during the connection time and unusable by on-top media applications. The interruptions of content transmissions not only lead to the failure of media presentations to users, but the transmission of the invalid fragment contents would also result in the significant waste of precious vehicular bandwidth. On addressing this issue, in this work we target on provisioning the integrity-oriented inter-vehicle content transmissions. Given the initial distance and mobility statistics of vehicles, we develop an analytical framework to evaluate the data volume that can be transmitted upon the short-lived and spotty V2V connection from the source to the destination vehicle. Provided the content file size, we are able to evaluate the likelihood of successful content transmissions through the model. Based upon this analysis, we propose an admission control scheme at the transmitters, that filters the suspicious content transmission requests which are unlikely to be accomplished over the transient inter-vehicle links. Using extensive simulations, we demonstrate the accuracy of the developed analytical model, and the effectiveness of the proposed admission control scheme. In the simulated scenario, with the proposed admission control scheme applied, it is observed that about 30% of the network bandwidth can be saved for effective content transmissions.**

I. Introduction

By equipping vehicles with on-board wireless transceivers, the newly emerged vehicular ad hoc networks (VANETs) enable vehicles on the road to wirelessly communicate with each other and to the roadside gateways for Internet access using the exclusive DSRC (dedicated short-range communications) radio spectrum [1]. Over this new paradigm of networking, a variety of novel and exciting media applications, such as instant message, video streaming and social networking, *etc.*, can be delivered to fleet travelers on the road to make their trips more efficient and enjoyable.

In this work, we focus on provisioning the efficient media applications in highway vehicular networks through the framework of integrity-oriented content transmissions. Specifically, in media applications, it is basic to transform information into the form of digital files for transmissions, such as text messages, images, video/audio clips. Media communications in VANETs typically boil down to the consecutive transmissions of heterogeneous-sized media content files from the source to the destination[1] [2]. Furthermore, in order to ensure the successful presentation of on-top media applications, digital contents are required to be fully transmitted in their entirety; fragment or partially transmitted contents are unusable by typical applications. In real-world deployments, the transmissions of fragment contents due to the network interruptions are not only annoying to end users with the deferred response or even failed presentation, but also significantly waste the network bandwidth with invalid data transmissions.

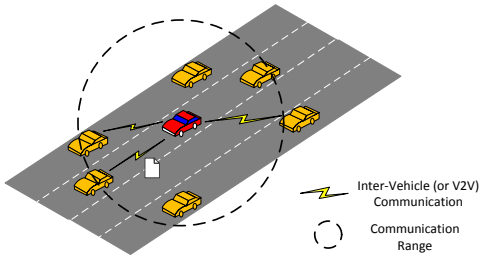

Fig. 1. Inter-vehicle communications on the highway

The issue of fragment contents tends to be even severe in highway vehicular networks. Notably, unlike the densely populated urban area where large-scale infrastructure could be available to provide the ubiquitous Internet access to vehicles [3], [4], the high-rate ubiquitous infrastructure connections on the highway is, however, not practical or very expensive due to the huge deployment and maintenance cost in the sparsely populated region [5], [6]. This makes the efficient use of infrastructure-less V2V communications the key for successful media communications, as a typical scenario shown in Fig. 1. Nevertheless, the inter-vehicle or V2V communications are highly dynamic and unreliable due to the following three factors, which make the effective inter-vehicle content transmissions very challenging:

- ▷ **Transient Connectivity**: with the diverse velocities of vehicles, the distance between vehicles is dramatically changing over time, resulting in the short-lived and intermittent V2V connectivity. For example, it is observed

[1]The on-top media application may constitute only one file, such as a MP3 or video clip, or request the transmission of a mixture of content files with different types, *e.g.*, a MySpace blog contains texts, images and video clips

that the average connection time among vehicles on the highway in a real-world measurement is only around 15 seconds [5].

- ▷ **Harsh Wireless Channel**: due to the high mobility, severe Doppler shift and absence of line-of-sight communications[2], the V2V channel suffers from severe fading and channel impairments. As reported in [8], the throughput of V2V communications in a real-world measurement is less than one fifth of the throughput of the vehicle-to-infrastructure communication.
- ▷ **Intense Channel Contention**: the vehicular network is typically large-scale with a multitude of vehicles sharing (or contending) the channel simultaneously. For example, as indicated in [9] a stable highway traffic flow typically constitutes $20 \sim 30$ vehicles per mile per lane. In other words, in an eight-lane bidirectional highway section with smooth traffic flow and V2V communication range to be around 300 meters, approximately $30 \sim 45$ vehicles will share the channel for transmissions at the same time.

Note that a typical content file, such as a MP3 or video clip, is of several MBs, which may take tens of seconds or several minutes to transmit at the rate of several tens or hundreds Kbps. Over the short-lived and spotty V2V channel as discussed above, content transmissions can hardly be accomplished if without a careful design, leading to poor system performance with rampant fragment contents and invalid transmissions.

In this work, we unfold our journey in three steps towards the integrity-oriented content transmission. First, we focus on the content transmissions between a randomly selected source-destination pair of vehicles on the highway, and develop an analytical model to evaluate the data transmission performance in terms of the data volume that can be transmitted during the transient connection time of selected vehicles. Our analysis comprises of three components on the modeling of headway distance between vehicles, wireless channel fading and MAC contentions, respectively, and represent the data transmission performance as a function of the initial headway distance between the source-destination pair and the statistics of velocities. Based on the developed model, we are able to evaluate the likelihood of successful content transmission during the short-lived V2V connection. After that, we propose an adaptive admission control scheme to manage the content transmission subscriptions among vehicles. Using our proposal, the file transmissions which can hardly be finished during the short-lived V2V connections will be rejected before the transmission commences. This thus prevents the potential bandwidth waste and invalid transmissions. Lastly, using extensive simulations, we show the accuracy of the developed model and validate the effectiveness of the proposed admission control protocol.

The remainder of this paper is organized as follows: Section II provides a brief survey on the existing literature and highlights our contributions in the light of related works. Section III presents the mathematical model on evaluating the download performance of contents over the dynamic and transient V2V connections. Based on the model developed in Section III, Section IV proposes the admission control scheme targeting to avoid the invalid content transmissions. Section V conducts extensive simulations to validate the accuracy of the analysis and the effectiveness of the proposed protocol, and Section VI closes this paper with concluding remarks.

[2]With the heterogenous heights and shapes of vehicles, the line-of-sight link could be blocked by intermediate vehicles as obstacles on the highway [7].

II. Related Literature

The surge of media and content distribution applications in the Internet, such as Youtube, MySpace and Netflix, has motivated the extensive research efforts on the design of efficient highway vehicular content distribution/transmission networks. For instance, Li *et al.* [10] investigate on multicasting the popular multimedia contents to a vast of interested vehicles on the highway with the symbol-level network coding scheme applied. Under the similar framework of [10], Yan *et al.* [11] develop an analytical model to evaluate the multihop transmission throughput of the highway vehicular content distribution network. Zhang *et al.* [12] propose a platoon-based content replication schemes to enhance the data access performance in highway vehicular networks. Unlike [10], [11], [12] which investigate from a global system viewpoint and target to coordinate the content replications and distributions in the entire system, we focus on the microscopic performance of vehicular communications by investigating on the single-hop file transmission between a specific pair of vehicles.

Motivated by the challenges of severe network dynamics, a collection of papers have been devoted to the model and analysis of link performance and multi-hop connectivity in highway vehicular networks. Similar to our work, Yan *et al.* [13] also develop a model on the distribution of the V2V connection time on the highway. Given the initial distance among vehicles which is assumed to follow the log-normal distribution, [13] evaluates the traveled distance of source and destination vehicles within a given period, and accordingly computes the transmission distance and link connectivity after the given period. In comparison, our analysis does not rely on assumptions of the initial distance among vehicles and car following models. Zhang *et al.* [14] and Zhuang *et al.* [15], respectively, analyze the multi-hop connectivity of vehicles on the highway with the assumptions of Poisson distributed locations and static relative inter-vehicle distance. In our work, we consider the time-varying vehicle mobility and headway distance. Moreover, [14] and [15] consider the transmissions of safety messages which are typically very short in length. In this case, the packet-level performance in terms of packet transmission delay and loss probability is concerned which is studied in [16]. In contrast to that, we consider the transmission of media content files which are typically of several MBs and thus take much more time to transmit. As such, the session-level performance in terms of the integrity and finishing time of entire content transmission is more important. To the best of our knowledge, this paper represents the first theoretical work on evaluating the session-level performance in V2V communications.

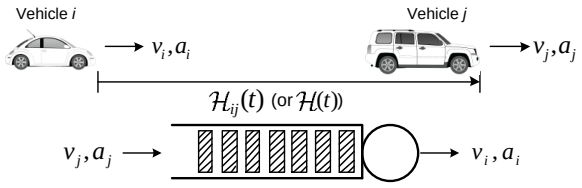

Fig. 2. Model of headway distance from i to j

III. System Model

We investigate on the highway vehicular network, where all the vehicles move over a linear topology. In particular, we focus on the content transmission between a randomly selected pair of vehicles, namely i and j. Our goal is to evaluate the impacts of network dynamics, from the aspects of transient connection time, channel fading and MAC contentions, on the data transmission performance from i to j in terms of the data volume that can be transmitted along the short-lived, spotty V2V channel. Our analysis is proceeded in four steps as following :

- Step 1: Headway distance prediction to estimate $\mathcal{H}_{ij}(t)$ which denotes the headway distance from i to j after duration t starting when the evaluation is initiated.
- Step 2: Channel fading analysis to evaluate the physical layer capacity, denoted by $\mathcal{C}_{ij}$, between i and j. At a given time, $\mathcal{C}_{ij}$ is a function of the headway distance $\mathcal{H}_{ij}(t)$ and is subject to the fast channel fading.
- Step 3: Channel contention model to derive the effective transmission rate from i to j, denoted by $\mathcal{R}_{ij}$, at the MAC layer after the channel contentions. $\mathcal{R}_{ij}$ is the MAC throughput dependent on the underlying physical layer transmission rate $\mathcal{C}_{ij}$ and number of vehicles sharing the channel.
- Step 4: Download Performance Evaluation to evaluate the data volume, denoted by $\mathcal{A}_{ij}$, that can be transmitted from i to j by integrating the MAC throughput $\mathcal{R}_{ij}$ over the V2V connection time.

In what follows, we derive the expressions of $\mathcal{H}_{ij}(t)$, $\mathcal{C}_{ij}$, $\mathcal{R}_{ij}$ in sequence and finally evaluate $\mathcal{A}_{ij}$. As $\mathcal{H}_{ij}(t)$ is a function of time, $\mathcal{C}_{ij}$ and $\mathcal{R}_{ij}$ also change over time. In brief of notation, we drop the subscript ij in the rest part of this section.

A. Headway Distance Prediction

We consider the headway distance $\mathcal{H}(t)$ as a directional variable from the source vehicle i to the destination vehicle j, as shown in Fig. 2. $\mathcal{H}(t) \geq 0$ if vehicle i is behind vehicle j in the moving direction; otherwise, $\mathcal{H}(t) < 0$. We model the headway distance from vehicle i to j as a $G/G/1$ queue, with each element of the queue size to be one meter, and the instantaneous queue length represents the current headway distance between the two vehicles.

The evolvement of queue length is subject to the movement of vehicles i and j. Let v_i and v_j denote the mean velocity of vehicles i and j, respectively. Let a_i and a_j denote the variance of vehicle i and j's velocities, respectively. In other words, v_j and a_j represent the mean and variance of the (meter) arrival rate to the queue, and v_i and a_i represent the mean and variance of the (meter) service rate of the queue. By applying the $G/G/1$ model, we implicitly assume that the movement, *i.e.*, the traveled distance of vehicles i and j, respectively, in the unit time is independent and identically distributed (i.i.d.), and is uncorrelated to that of each other. This is a working assumption in the multi-lane highway scenario with smooth and stable traffic. Notably, in the multi-lane highway with light traffic, vehicles i and j are free to adapt their velocities through accelarations/decelarations and lane changing which are subject to individual's driving habit [17]. In the case of the heavy traffic, as reported in [18], the headway distance between vehicles follows the Gaussian distribution which is related to the safety distance of different drivers. Moreover, for the ease of analysis, in this work, we consider the simple scenario in which the mobility of vehicles is stable in that the mean and variance of velocities are not changing over time. The assumption is practical as the variations of vehicle velocity on the highway are in a much larger time scale than the data transmissions.

We resort to the diffusion approximation [19] to evaluate the transient queue length, *i.e.*, instantaneous headway distance $\mathcal{H}(t)$ between the two vehicles. The headway distance $\mathcal{H}(t)$ is modeled as a one-dimensional Wiener process (or Brownian motion) with the drift $\mu = v_j - v_i$ and variance $\sigma = a_j + a_j$. As such, within the infinitesimal interval Δt, the increment of $\mathcal{H}$ is normally distributed as

$$\Delta\mathcal{H}(t) = \mathcal{H}(t+\Delta t) - \mathcal{H}(t) = \mu\Delta t + \Theta\sqrt{\sigma\Delta t} \quad (1)$$

with Θ denoting the random variable following the unit normal distribution.

Let r denote the initial headway distance from vehicle i to vehicle j upon the time instant when the headway distance estimation, *i.e.*, $\mathcal{H}(0) = r$ is initiated. Let $f_H(x;r,t)$ denote the probability density function (pdf) of $\mathcal{H}(t)$ at time t, conditional on the initial queue length, and

$$f_H(x;r,t) = \Pr\{x \leq \mathcal{H}(t) \leq x + \Delta x | \mathcal{H}(0) = r\}.$$

With the model in (1), $f_D(x,r,t)$ can be characterized by the Kolmogorov equation (alternatively known as Fokker–Planck equation) as

$$\frac{1}{2}\sigma\frac{\partial^2}{\partial x^2}f_H(x;r,t) + \mu\frac{\partial}{\partial x}f_H(x;r,t) = \frac{\partial}{\partial t}f_H(x;r,t) \quad (2)$$

subject to the initial condition of the headway distance,

$$f_H(x;r,0) = \delta(r), \quad (3)$$

with $\delta(\cdot)$ denoting the Dirac delta function.

Solving (2), we have [19]

$$f_H(x;r,t) = \frac{1}{\sqrt{2\pi\sigma t}}\exp\left\{-\frac{(x-r-\mu t)^2}{2\sigma t}\right\} \quad (4)$$

Eqn. (4) represents the distribution of $\mathcal{H}(t)$ over time t provided the initial headway distance r and the statistics of vehicle velocity, and $f_H(x;r,t)$ follows the normal distribution

with the mean $r+\mu t$ and variance σt.

B. Model of Wireless Channel Fading

Given the headway distance between the source and destination vehicles, we are ready to evaluate the physical layer transmission rate between them.

The vehicular communications operate on the exclusive DSRC frequency band between 5.850 to 5.925 GHz as mandated by US FCC. The 75 MHz DSRC spectrum is divided into seven 10 MHz channels with the rest 5 MHz reserved for future use. Of the seven channels, four channels can be used for the IP-based infortainment applications, with two channels intended for medium-range communication with the maximum transmit power to be 33 dBm, and another two channels for short-range communication with the maximum transmit power to be 23 dBm (for private vehicles) [20]. Over each channel, the physical layer operation of the vehicular communication is specified by the IEEE 802.11p standard, which adopts OFDM (Orthogonal Frequency Division Multiplexing) and works in the same manner of IEEE 802.11a physical layer. Four different modulation schemes (BPSK, QPSK, 16-QAM and 64-QAM) and three different FEC coding rates ($1/2, 2/3$ and $3/4$) are enabled, which leads to eight different transmission rates from 3 Mbps to 27 Mbps as shown in Table I.

In this paper, we adopt the measurement results in [21] to evaluate the physical layer capacity of V2V communications. In specific, let d denote the distance between vehicle i and j at time t, and $d=|\mathcal{H}(t)|$. The received signal strength as a function of d can be represented by the dual-slope piecewise-linear model [21], as

$$P(d)=\begin{cases} P(d_0)-10\alpha_1\log_{10}\left(\frac{d}{d_0}\right)+\chi_{\sigma_1}, & d_0\le d\le d_c \\ P(d_0)-10\alpha_1\log_{10}\left(\frac{d_c}{d_0}\right)-10\alpha_2\log_{10}\left(\frac{d}{d_c}\right)+\chi_{\sigma_2}, & d>d_c \end{cases} \tag{5}$$

where $P(d_0)$ is the known signal strength at the reference distance d_0. α_1 and α_2 are the path loss exponents. d_c is the critical distance which can be evaluated as $d_c=\frac{4a_ia_j}{\lambda}$ with a_i, a_j denoting the antenna heights of vehicles i and j, respectively, and λ denoting the wavelength of the electromagnetic wave at 5.9 GHz. χ_{σ_1} and χ_{σ_2} zero-mean normally distributed random variables with the standard deviations σ_1 and σ_2, respectively.

Eqn. (5) characterizes the path loss and shadowing effects of the channel. Due to the typically short-range connections of V2V communications, a more accurate representation of the channel is to identify the fast fading. As reported in [21], the fast fading tends to be Rician at a short distance, and become severe as distance increases due to the gradual loss of the line-of-sight communication. Let s be a random variable, denoting the the received signal envelope in the fast fading at vehicle j. The pdf of s can be represented by the Nakagami(m,Ω) distribution as

$$f_s(x;m,\Omega)=\frac{2m^m}{m^m\Gamma(m)}r^{2m-1}\exp\left(-\frac{m}{\Omega}x^2\right) \tag{6}$$

where Ω is the average received power before the envelop detection which can be evaluated as $\Omega=E[P(d)]$ with $P(d)$ shown in (5). m is the fading parameter. For $m=1$, (6) reduces to Rayleigh distribution, and for $m=\frac{(K+1)^2}{2K+1}$, (6) becomes the Ricean fading with parameter K. $\Gamma(x)=\int_0^\infty e^{-t}t^{x-1}dt$ is the Gamma function. With (6), the cumulative density function (cdf) of the received power s^2 at vehicle j is

$$\Pr\left\{s^2\le x\right\}=1-\frac{\Gamma\left(m,\frac{m}{\Omega}x\right)}{\Gamma(\mu)} \tag{7}$$

where $\Gamma\left(m,\frac{m}{\varpi}x\right)=\int_{\frac{m}{\varpi}x}^\infty y^{\mu-1}\exp(-y)\,dy$.

With (7), the CDF of the signal to noise ratio (SNR) at the receiver is

$$\Pr\left\{\frac{s^2}{\varphi}\le x\right\}=1-\frac{\Gamma\left(m,\frac{m}{\Omega}\varphi x\right)}{\Gamma(m)}, \tag{8}$$

where φ denotes the thermal noise power at the receiver.

We adopt the model in [22] to evaluate the channel modulation. In specific, we assume that the on-board wireless transceiver supports κ discrete modulation rates, denoted as $\Theta=\{c_1,c_2,\cdots,c_\kappa\}$ with $c_1<c_2<\cdots<c_\kappa$, and the transmission rates are adapted in the SNR-triggered manner. Specifically, each modulation rate, say c_k, is associated with a predefined threshold, say ϑ_k, where $\vartheta_{\kappa+1}$ is set ∞. The transmission rate c_k is adopted in the physical layer if the current SNR is above ϑ_k and smaller than ϑ_{k+1}. As such, based on (8), provided the distance of communication, the transmission rate c_k is selected with the probability

$$\begin{aligned}\Pr\{\mathcal{C}=c_k\}=&\Pr\left\{\vartheta_k<\frac{s^2}{\varphi}\le\vartheta_{k+1}\right\} \quad \text{for } 1\le k\le\kappa-1\\ =&\frac{1}{\Gamma(\mu)}\left(\Gamma\left(m,\frac{m}{\Omega}\varphi\vartheta_k\right)-\Gamma\left(m,\frac{m}{\Omega}\varphi\vartheta_{k+1}\right)\right),\\ \Pr\{\mathcal{C}=c_k\}=&\frac{\Gamma\left(m,\frac{m}{\varpi}\varphi\vartheta_\kappa\right)}{\Gamma(m)} \qquad \text{for } k=\kappa,\end{aligned} \tag{9}$$

and with the rest probability

$$\Pr\{\mathcal{C}=0\}=1-\sum_{k=1}^{\kappa}\Pr\{\mathcal{C}=c_k\}.$$

C. Channel Contention Model

The vehicular networks adopt the contention-based MAC to resolve the channel contentions among parallel transmissions. In this part, we evaluate the MAC throughput $\mathcal{R}$ from i to j.

Let $\mathcal{N}$ denote the number of vehicles, including vehicle i, which are contending the channel for transmissions in the highway section. We assume that $\mathcal{N}$ follows the Poisson distribution as

$$f_n(\mathcal{N})=\frac{(\rho S)^{\mathcal{N}}}{\mathcal{N}!}\exp(-\rho S) \tag{10}$$

where ρ is the traffic density, defined as vehicles per meter. S denotes the carrier sensing range of vehicles. The Poisson distribution of vehicles on the highway has been reported in [23] based on the analysis of real-world trace. This model is also widely used in literature, *e.g.*, [14].

We assume that the IEEE 802.11b DCF (distributed coordination function) scheme is applied for the MAC scheduling

with the RTS/CTS scheme adopted to eliminate the hidden terminals of transmissions. Let W denote the minimum contention window size used in the exponential backoff of vehicle i. Let τ denote the average transmission probability of each vehicle, and

$$\tau = \frac{1}{W/2+1}. \tag{11}$$

The probability of the successful transmission from vehicle i to vehicle j, given that the vehicle i transmits, is

$$P_{\rm suc} = (1-\tau)^{\mathcal{N}-1}. \tag{12}$$

The MAC throughput from vehicle i to vehicle j is therefore

$$\mathcal{R} = \tau P_{\rm suc} \frac{{\rm FL}_i}{T} \tag{13}$$

where ${\rm FL}_i$ is the frame/packet length of vehicle i, including the payload and the packet header. T is the average length of a time slot in DCF, mathematically

$$T = (1-P_{\rm tran})\,{\rm SlotTime} + (P_{\rm tran}-P_{\rm suc})\,T_{\rm cld} + P_{\rm suc}T_{\rm suc},$$

where $P_{\rm tran}$ is the probability that the channel is busy for transmission and $P_{\rm tran} = 1-(1-\tau)^n$. $P_{\rm suc}$ is the probability of successful transmission when channel is busy, and $P_{\rm suc} = n\tau(1-\tau)^{n-1}$. $T_{\rm cld}$ and $T_{\rm suc}$ are the average time of collided and successful transmissions, respectively. Mathematically, we have

$$\begin{cases} T_{\rm cld} = {\rm RTS} + {\rm DIFS} + {\rm SlotTime}, \\ T_{\rm suc} = {\rm RTS} + 3\times{\rm SIFS} + 4\times{\rm SlotTime} + {\rm CTS} \\ \qquad\quad + \dfrac{E({\rm FL})}{E(C)} + {\rm ACK} + {\rm DIFS}, \end{cases} \tag{14}$$

where SlotTime is the unit slot time of DCF backoff. SIFS and DIFS are predefined time intervals reserved for the DCF signallings and operations. RTS, CTS and ACK represent the time interval of RTS, CTS and ACK transmissions, respectively. Here, we assume that the RTS/CTS scheme is adopted with DCF to eliminate the hidden terminals during the transmission.

$E({\rm FL})$ in (14) is the average frame length, including the payload and packet header, of transmissions. Given that $\mathcal{N}$ vehicles are contending the channel, we have

$$E({\rm FL}) = \frac{1}{\mathcal{N}}{\rm FL}_i + \frac{\mathcal{N}-1}{\mathcal{N}}\widehat{\rm FL}, \tag{15}$$

with $\widehat{\rm FL}$ being the average frame length of the other vehicles. In this work, we assume that the frame length of different vehicles follow the same and known distribution.

$E(C)$ in (14) is the average physical layer transmission rate of vehicles. Given the transmission rate of vehicle i to be $\mathcal{C}$, we have

$$E(C) = \frac{1}{\mathcal{N}}\mathcal{C} + \frac{\mathcal{N}-1}{\mathcal{N}}\widehat{C}, \tag{16}$$

where $\widehat{C}$ is the average transmission rate of the other vehicles. We assume that transmission distance among each source destination pair in the network is uniformly distributed[3] within the carrier sensing range S, and accordingly

$$\widehat{C} = \frac{1}{S}\int_0^S c_k \Pr\{\mathcal{C} = c_k\}\,dx. \tag{17}$$

D. Data Download Evaluation

We are now ready to evaluate the data amount $\mathcal{A}$ that can be transmitted from vehicle i to vehicle j. Within a time period of Υ ($\Upsilon \geq 0$), the integrated data volume transmitted from i to j is evaluated by integrating the MAC throughput $\mathcal{R}$ over the range $[0,\Upsilon]$ as

$$\mathcal{A} = \int_0^\Upsilon \mathcal{R}dt. \tag{18}$$

Note that (18) involves the integration over a random process. To simplify the analysis, we only derive the mean and an upper bound of the variance of $\mathcal{A}$ as

$$\mathbb{E}(\mathcal{A}) = \int_0^\Upsilon \mathbb{E}(\mathcal{R})\,dt \tag{19}$$

where

$$\mathbb{E}(\mathcal{R}) = \int_{-\infty}^{\infty}\sum_{n=1}^{\infty}\sum_{k=1}^{\kappa} P(\mathcal{C}=c_k)\,\mathcal{R}f_n(\mathcal{N})\,f_H(x;r,t)\,dx,$$

and

$$\mathbb{V}(\mathcal{A}) \leq \Upsilon\int_0^\Upsilon \mathbb{E}\left(\mathcal{R}^2\right)dt - \mathbb{E}(\mathcal{A})^2, \tag{20}$$

where

$$\mathbb{E}\left(\mathcal{R}^2\right) = \int_{-\infty}^{\infty}\sum_{n=1}^{\infty}\sum_{k=1}^{\kappa} P(\mathcal{C}=c_k)\,\mathcal{R}^2 f_n(\mathcal{N})\,f_H(x;r,t)\,dx.$$

The derivations of (19) and (20) are shown in the Appendix.

IV. Call Admission Control

In in this section, we devise an admission control scheme at source vehicles to prevent content transmissions which are unlikely to be finished within the short-lived connection time.

Let F_{ij} denote the file size to be transmitted from vehicle i to vehicle j. Before the file transmission, we assume that a three-tuple $\{{\rm Location}_j, v_j, a_j\}$ is notified to vehicle i by vehicle j, piggybacked by the download request of vehicle j, where ${\rm Location}_j$ is the GPS location of vehicle j. As such, before the mass file transmission, vehicle i first examines the following inequality as

$$\Pr\{\mathcal{A} > F_{ij}\} > \xi, \tag{21}$$

where ξ is predefined and $0 << \xi < 1$. If (21) can be satisfied, which indicates that the content transmission can be completed with high probability, the download request of vehicle j will be approved with ensuing data transmissions from i to j. Otherwise, the download request will be rejected so as to prevent the potential transmission of fragment contents and avoid waste of bandwidth.

[3]This also implies that the content transmissions among vehicles are independent of their distance.

As the distribution of $\mathcal{A}$ is unknown, we apply the Chebyshev inequality to relax (21). According to the one-sided Chebyshev inequality, we have

$$\Pr\{\mathcal{A} \leq F_{ij}\} \leq \frac{\mathbb{V}(\mathcal{A})}{\mathbb{V}(\mathcal{A}) + [\mathbb{E}(\mathcal{A}) - F_{ij}]^2} \quad (22)$$

with $F_{ij} < \mathbb{E}(\mathcal{A})$.

By substituting (20) and (22) into (21), we have that (21) can be satisfied if the following inequality is satisfied

$$\frac{\Upsilon \int_0^{\Upsilon} \mathbb{E}(\mathcal{R}^2)\, dt - \mathbb{E}(\mathcal{A})^2}{\Upsilon \int_0^{\Upsilon} \mathbb{E}(\mathcal{R}^2)\, dt - \mathbb{E}(\mathcal{A})^2 + [\mathbb{E}(\mathcal{A}) - F_{ij}]^2} \leq 1 - \xi, \quad (23)$$

where Υ is a predefined scalable, representing the deadline of content transmission required by the applications at the receiver j.

By implementing (23) in the admission control, the request of content transmission is approved by vehicle i if both of the following conditions are met: 1) $F_{ij} < \mathbb{E}(\mathcal{A})$, and 2) (23) is satisfied. Note that as (22) overestimates $\Pr\{\mathcal{A} \leq F_{ij}\}$, the resultant admission control scheme is more conservative than that adopts (21). Moreover, using an upper bound of $\mathbb{V}(\mathcal{A})$ as represented by (20) in (23) will also make the admission control scheme conservative.

V. Simulations

In this section, we examine the accuracy of the analytical model and effectiveness of the proposed admission control scheme using simulations.

A. Simulation Setup

Our simulations are based on a customer simulator coded in C++, which is adapted from [24], [25]. In each simulation run, we simulate file transmissions among vehicles on a linear highway topology with the following configurations:

Vehicle Mobility: We simulate 1000 vehicles in a highway road section. At the commencement of each simulation run, vehicles are placed on the road following Poisson distribution; the headway distance between neighboring vehicles follows the exponential distribution with mean value of 60 meters. The initial density of vehicles is thus $\rho = 1/60$ car/m. When the simulation proceeds, vehicles adapt their velocity at each unit time following Normal distribution with the mean value uniformly distributed within $[70, 130]$ km/h and the standard deviation uniformly distributed within $[21, 39]$ km/h. A similar configuration of vehicle mobility is also used in [17].

File Transmission: Along its trajectory, each vehicle iteratively requests data files to download from the neighboring vehicles. In specific, upon each iteration of file transmission, a vehicle (as receiver) first randomly selects a source node from its one-hop neighbors within the communication range of 300 meters. The selected source node then generates a content file with the size uniformly distributed within the range $[1, 10]$ MB and transmit to the receiver vehicle over the DSRC radio. The file is transmitted in a packet flow with the frame length FL following the distribution as $P(\text{FL}) = 0.2 \times \delta(\text{FL} - 200) + 0.25 \times \delta(\text{FL} - 800) + 0.35 \times \delta(\text{FL} - 1200) + 0.2 \times \delta(\text{FL} - 1500)$. The file transmission terminates if either one of the following three events occurs: 1. the entire file has been transmitted successfully to the receiver; 2. the receiver vehicle moves outside the communication range (*i.e.*, 300 meters) of the source vehicle; 3. a deadline of content transmission $\Upsilon = 100$s is reached. The termination of a file transmission then initiates a new iteration of file transmission following the same procedure as above.

TABLE I
DSRC Data Rate and SNR Threshold

SNR Threshold (dB)	5	6	8	11	15	20	25	N/A
Data Rate (Mbps)	3	4.5	6	9	12	18	24	27

TABLE II
Fading Parameter m over Distance d (in meter)

d	≤ 5.5	≤ 13.9	≤ 35.5	≤ 90.5	≤ 230.7	≤ 588
m	4.07	2.44	3.08	1.52	0.74	0.84

Channel Fading: Each vehicle is equipped with a single transceiver operating on the DSRC radio. Based on the value of received SNR, the transmitter adapts the modulation scheme and physical layer transmission rate according to SNR thresholds shown in Table I [26]. The thermal noise power is set to be -96 dBm which is same as [24]. The received signal is deteriorated by the Nakagami-m fading as (6). In (6), the fading parameter m is a function of the transmission distance is based on the measurement in [21] as shown in Table II. The average received power is determined by (5) in which $\alpha_1 = 2.1$, $\alpha_2 = 3.8$ based on [21] and the received power at reference distance $d_0 = 100$m is evaluated by the two-ray ground reflection model as $P(d_0) = P_t G_t G_r \frac{h_t^2 h_r^2}{d_0^4 L}$ with the transmission power $P_t = 23$ dBm (short-range), gain of the transmitter (receiver) antenna $G_t = 1$ ($G_r = 1$), height of the transmitter (receiver) antenna $h_t = 1$m ($h_r = 1$m) and system loss factor $L = 1$.

MAC Contention: The channel access of packet transmissions is scheduled by the DCF MAC with RTS/CTS handshake. The minimum contention window of vehicles is set to be $W = 32$, and the carrier sensing range S is sent to be 500 meters. Other MAC layer parameters are as follows: SlotTime $= 13\mu s$, SIFS $= 32\mu s$, DIFS $= 32\mu s$, RTS transmission time $= 53\mu s$, CTS transmission time $= 37\mu s$ and ACK transmission time $= 37\mu s$.

B. Distribution of Headway Distance

In the first experiment, we validate the accuracy of (4) on predicting of the distribution of headway distance after time period t. To achieve this goal, we insert two vehicles i and j (assuming i transmits to j) into the network with the controllable initial headway distance r and velocities. Unless otherwise mentioned, we set $v_i = 97.2$ km/h, $a_i = 30.6^2$ and $v_j = 90$ km/h, $a_j = 27^2$ in this experiment. The averaged

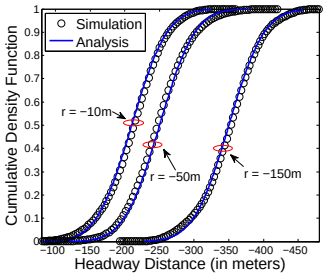

Fig. 3. CDF of $\mathcal{H}_{ij}(t)$ at $t = 100$s with different initial headway distance r

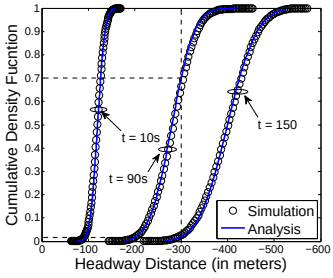

Fig. 4. CDF of $\mathcal{H}_{ij}(t)$ with initial headway distance $r = -100$m at different time t

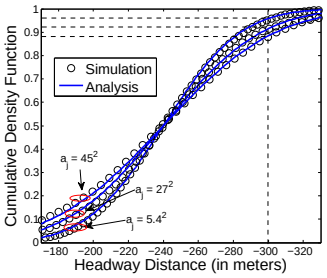

Fig. 5. CDF of $\mathcal{H}_{ij}(t)$ at $t = 100$s and $r = -100$m with different a_j

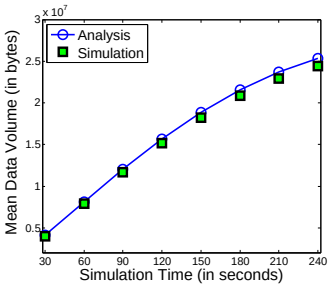

Fig. 6. Mean data volume transmitted from i to j until the simulation time

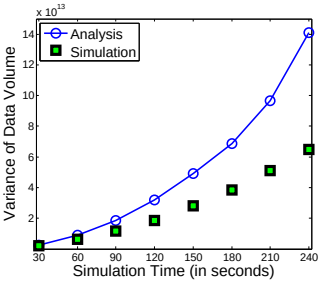

Fig. 7. Variance of the data volume transmitted from i to j until the simulation time

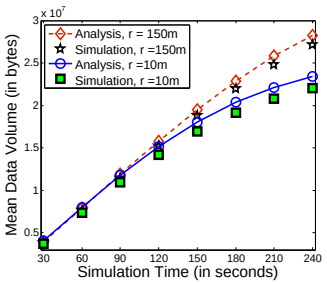

Fig. 8. Variance of the data volume transmitted from i to j until the simulation time with different r at $t = 0$

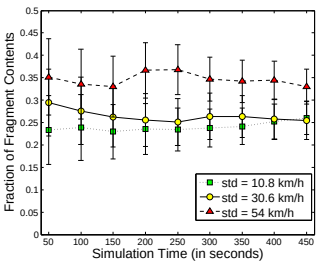

Fig. 9. Fraction of fragment contents in the overall data volume transmitted with different standard deviation of the selected vehicle

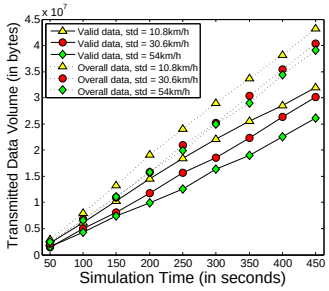

Fig. 10. Valid and overall data volume transmitted

results over 300 simulation runs are reported and compared with the analysis derived from (4).

Fig. 3 shows the CDF of the headway distance $\mathcal{H}(t)$ when $t = 100$s with the different values of initial distance r. By increasing r, it can be seen that the curves shift to the right hand side, indicating the increasing mean value of $\mathcal{H}(t)$. The variance of $\mathcal{H}(t)$ is not related to r as indicated by (4) and simulations. Fig. 4 shows the CDF of $\mathcal{H}(t)$ at different time t with $r = -100$m (*i.e.*, vehicle i is ahead of vehicle j in the moving direction). It can be seen that by increasing t, both the mean and variance of $\mathcal{H}(t)$ increase. With the communication range of vehicles typically to be 300m, from Fig. 4, it can be seen that at $t = 90$s, the probability that vehicles i and j are connected is 0.7 and this probability reduces to almost 0 when $t = 150$s. Fig. 5 shows the CDF of $\mathcal{H}(t)$ with different a_j (variance of vehicle j's velocity). By increasing a_j, vehicle j adapts its velocity more intensively over time. This accordingly leads to the increased variance of $\mathcal{H}(t)$ and reduced probability of connection between i and j with fixed r as indicated by Fig. 5.

C. Download Performance during Connection Time

In the second experiment, we investigate on the accuracy of (19) and (20) on evaluating the mean and variance of the transmitted data volume among vehicles. To this end, we investigate on the same pair of vehicles i and j in the previous experiment and let vehicle i transmit to vehicle j with the packet length to be 1000 bytes. We report the averaged results over 300 simulation runs and compare the analysis derived from (19) and (20).

Fig. 6 shows the mean data volume that can be transmitted from vehicle i to vehicle j as a function of time when the initial headway distance from vehicle i to vehicle j is $r = 50$m. The data volume at each instant represents the data transmitted from time 0 until the corresponding time instant. As we can see from Fig. 6, with the time increasing, the mean volume of transmitted data increases as download time increases whereas the rate of increment reduces. This is because that as time elapses, the distance between i to j increases and the transmission rate of vehicle i reduces accordingly. Fig. 6 shows the variance of the data volume that can be transmitted from vehicle i to vehicle j when $r = 50$m. Note that (20) represents an upper bound of $\mathbb{V}(\mathcal{A})$. As we can see from Fig. 7, with time increasing, the gap of the bound increases. This is because that the error of estimation accumulates over time. Fig. 8 shows the mean data volume transmitted from i to j with different values of initial distance r. As we can see, when $r = 150$m, more data can be transmitted compared with that with $r = 10$m. This is because that as $v_i > v_j$ the high-rate connection between i and j is longer in the case when $r = 150$m than that when $r = 10$m.

D. Validation of Call Admission Control

In the last experiment, we examine the effectiveness of the proposed admission control scheme. We investigate on a randomly selected vehicle node in the network and set the mean and standard deviation of its velocity to be 97.2 km/h and 30.6 km/h, respectively, unless otherwise mentioned. The selected vehicle continuously subscribes to download files from neighboring vehicles in the communication range following the file transmission behavior as aforementioned. The deadline of

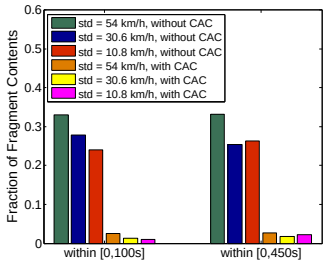

Fig. 11. Fraction of fragment contents with and without admission control (CAC) mechanism applied

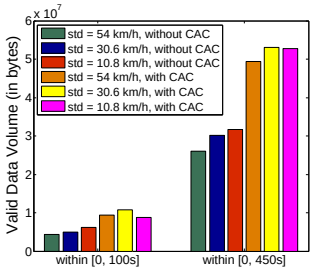

Fig. 12. Valid received data volume with and without admission control (CAC) mechanism applied

content transmission Υ in (23) is set to be 100s and ξ is set to be 0.9. In what follows, we show the download performance of the selected vehicle with and without the admission control mechanism applied, respectively.

Fig. 9 shows the fraction of fragment contents in the overall data volume transmitted when the admission control mechanism is not applied, with different standard deviations of the selected vehicle's velocity. As we can see in the simulated scenario, around 23% to 37% of the overall transmitted data are wasted for the delivery of fragment contents. By increasing the standard deviation of the selected vehicle's velocity, more fragment content transmissions are observed as in this case the mobility of the selected vehicle changes more intensively, leading to the more dynamic and unreliable V2V connections. Fig. 10 shows the overall data received by the selected vehicle, together with the valid data of entire content downloads, when the admission control scheme is not applied. Similar to Fig. 9, by increasing the standard deviation of the selected vehicle's velocity, we observe the decreased data volume received by the vehicle. This also attributes to the increase of channel dynamics due to the enhanced mobility.

Fig. 11 shows the fraction of fragment contents in the overall transmissions during the intervals of $[0, 100s]$ and $[0, 450s]$, respectively, with and without admission control applied. As we can see, with the admission control mechanism applied, the fraction of fragment contents downloaded is below 3% of the overall data received. With the stardard deviation of the selected vehicle's velocity reducing, the fraction of fragment contents downloaded reduces. Fig. 12 shows the valid data volume downloaded by the selected vehicle within the intervals of $[0, 100s]$ and $[0, 450s]$, respectively, with and without admission control applied. With the transmission of fragment contents dramatically reduced due to the admission control, the valid data receives increases around 50% to 60% of the case without admission control.

VI. Conclusion

We conclude the paper by emphasising that at the foundation of efficient vehicular communications lies the basic requirement of effective and efficient transmissions of *intact content files* to the highly mobile vehicles. Due to the dynamic nature of the volatile and spotty V2V channels, to guarantee the integrity of inter-vehicle content transmissions is very challenging but foremost and key to enable efficient media applications to vehicles. In this work, we have provided a theoretical treatment on provisioning the integrity-oriented content transmission, which, to the best of our knowledge, represents the first study in literature on this direction. To this end, we have developed a comprehensive analytical framework to evaluate the performance of data content transmissions over the dynamic V2V channel. The proposed model captures the node mobility, channel fading and MAC contentions in one framework, and has been verified by extensive simulations. Based on the proposed model, we have devised an admission control scheme at the transmitter to filter the transmission requests which are unlikely to be finished during the transient connection time. Using simulations, we have shown that the proposed scheme can help save around 30% of the network bandwidth in the simulated scenario.

We plan to extend the work in two dimensions in the future. Firstly, we plan to conduct field tests and investigate on the performance of the proposed analytical model and admission control mechanisms in the real-world scenarios. Secondly, we plan to extend the analysis of integrity-oriented content transmission to the multi-hop transmission scenario in which content files are transmitted through multiple V2V relays. As such, the data transmission performance not only relies on the mobility of source and destination vehicles, but are also dependent on that of the intermediate relays.

Appendix: Derivation of (19) and (20)

According to (18), we have

$$\mathbb{E}\left(\mathcal{A}\right) = \mathbb{E}\left(\int_0^{\Upsilon} \mathcal{R} dt\right) = \int_0^{\Upsilon} \mathbb{E}\left(\mathcal{R}\right) dt. \tag{24}$$

$\mathbb{E}\left(\mathcal{R}\right)$ can be derived based on the conditional expectation as

$$\mathbb{E}\left(\mathcal{R}\right) = \mathbb{E}_d \mathbb{E}_n \mathbb{E}_c \left(\mathcal{R}; \mathcal{N}, d\right) \tag{25}$$

where $\mathbb{E}_c\left(\cdot\right)$ is the expectation on the physical layer transmission rate. $\mathbb{E}_n\left(\cdot\right)$ is the expectation on the number of vehicles in the carrier sensing range. $\mathbb{E}_d\left(\cdot\right)$ is the expectation on the distance between vehicles i and j. Note that the distribution of $\mathcal{N}$ and d are independent.

Given (9), we have

$$\mathbb{E}_c\left(\mathcal{R}; \mathcal{N}, d\right) = \sum_{k=1}^{\kappa} P\left\{\mathcal{C} = c_k\right\} \mathcal{R}. \tag{26}$$

Given the Poisson distribution of $\mathcal{N}$ in (10)

$$\mathbb{E}_n \mathbb{E}_c \left(\mathcal{R}; \mathcal{N}, d\right) = \sum_{\mathcal{N}=1}^{\infty} \mathbb{E}_c \left(\mathcal{R}; \mathcal{N}, d\right) f_n\left(\mathcal{N}\right). \tag{27}$$

Given the distribution of the headway distance specified in (4), we have

$$\mathbb{E}_d \mathbb{E}_n \mathbb{E}_c \left(\mathcal{R}; \mathcal{N}, d\right) = \int_{-\infty}^{\infty} f_H\left(x; r, t\right) \mathbb{E}_n \mathbb{E}_c \left(\mathcal{R}; \mathcal{N}, |x|\right) dx. \tag{28}$$

Substituting (25), (26), (27) and (28) into (24), we have (19).

To derive (20), we have

$$\mathbb{V}\left(\mathcal{A}\right) = \mathbb{E}\left(\mathcal{A}^2\right) - \mathbb{E}\left(\mathcal{A}\right)^2. \tag{29}$$

where

$$\mathbb{E}\left(\mathcal{A}^2\right) = \mathbb{E}\left(\int_0^{\Upsilon} \mathcal{R}_t dt \int_0^{\Upsilon} \mathcal{R}_\tau d\tau\right) \tag{30}$$

with $\mathcal{R}_t$ and $\mathcal{R}_\tau$ following the same distribution as $\mathcal{R}$ at time t and τ, respectively.

To evaluate the integral in (30), we partition the time duration $[0, \Upsilon]$ into χ slots with each slot $\Delta t = \frac{\Upsilon}{\chi}$. According to the definition of Riemann integral, we have

$$\int_0^{\Upsilon} \mathcal{R}_t dt = \lim_{\chi\to\infty} \sum_{i=1}^{\chi} \mathcal{R}_{i\Delta t} \Delta t \tag{31}$$

In the similar manner, we have

$$\int_0^{\Upsilon} \mathcal{R}_\tau d\tau = \lim_{\chi'\to\infty} \sum_{j=1}^{\chi'} \mathcal{R}_{j\Delta\tau} \Delta\tau \tag{32}$$

with $\Delta\tau = \frac{\Gamma}{\chi'}$.

Substituting (31) and (32) into (30), we have

$$\begin{aligned}\mathbb{E}\left(\mathcal{A}^2\right) &= \lim_{\chi\to\infty}\lim_{\chi'\to\infty} \mathbb{E}\left(\sum_{i=1}^{\chi}\sum_{j=1}^{\chi'} \mathcal{R}_{i\Delta t}\mathcal{R}_{j\Delta\tau}\Delta t\Delta\tau\right) \\ &= \lim_{\chi\to\infty}\lim_{\chi'\to\infty} \left(\sum_{i=1}^{\chi}\sum_{j=1}^{\chi'} \mathbb{E}\left(\mathcal{R}_{i\Delta t}\mathcal{R}_{j\Delta\tau}\right)\Delta t\Delta\tau\right)\end{aligned} \tag{33}$$

Since $\mathcal{R}_{i\Delta t}$ and $\mathcal{R}_{j\Delta t}$ are positive real numbers, we have

$$\mathcal{R}_{i\Delta t}\mathcal{R}_{j\Delta\tau} \le \frac{1}{2}\left(\mathcal{R}_{i\Delta t}^2 + \mathcal{R}_{j\Delta\tau}^2\right).$$

Substituting it into (33), we have

$$\begin{aligned}\mathbb{E}\left(\mathcal{A}^2\right) &\le \lim_{\chi\to\infty}\lim_{\chi'\to\infty} \frac{1}{2}\sum_{i=1}^{\chi}\sum_{j=1}^{\chi'} \mathbb{E}\left(\mathcal{R}_{i\Delta t}^2 + \mathcal{R}_{j\Delta\tau}^2\right)\Delta t\Delta\tau \\ &= \lim_{\chi\to\infty}\lim_{\chi'\to\infty} \sum_{i=1}^{\chi}\sum_{j=1}^{\chi'} \mathbb{E}\left(\mathcal{R}_{i\Delta t}^2\right)\Delta t\Delta\tau \\ &= \Upsilon\int_0^{\Upsilon} \mathbb{E}\left(\mathcal{R}^2\right) dt\end{aligned} \tag{34}$$

where

$$\mathbb{E}\left(\mathcal{R}^2\right) = \int_{-\infty}^{\infty}\sum_{n=1}^{\infty}\sum_{k=1}^{\kappa} P\left\{\mathcal{C} = c_k\right\}\mathcal{R}^2 f_n\left(\mathcal{N}\right) f_H\left(x; r, t\right) dx$$

Substituting (34) into (29), we have (20).

REFERENCES

[1] H. T. Cheng, H. Shan, and W. Zhuang, "Infotainment and Road Safety Service Support in Vehicular Networking: From a Communication Perspective," *Mechanical Systems and Signal Processing*, vol. 25, no. 6, pp. 2020–2038, 2011.

[2] F. Bai and B. Krishnamachari, "Exploiting the Wisdom of the Crowd: Localized, Distributed Information-Centric VANETs," *IEEE Communications Magazine*, vol. 48, no. 5, pp. 138–146, Nov. 2010.

[3] V. Bychkovsky, B. Hull, A. Miu, H. Balakrishnan, and S. Madden, "A Measurement Study of Vehicular Internet Access Using In Situ Wi-Fi Metworks," in *Proc. of ACM Mobicom*, 2006.

[4] T. H. Luan, L. X. Cai, J. Chen, X. Shen, and F. Bai, "VTube: Towards the Media Rich City Life with Autonomous Vehicular Content Distribution," in *Proc. of IEEE SECON*, 2011.

[5] T. Zahn, G. O'Shea, and A. Rowstron, "Feasibility of Content Dissemination Between Devices in Moving Vehicles," in *Proc. of ACM CoNEXT*, 2009.

[6] Y. Zhuang, J. Pan, V. Viswanathan, and L. Cai, "On the Uplink MAC Performance of A Drive-Thru Internet," *IEEE Transaction on Vehicular Technology*, vol. 11, no. 4, pp. 1925 – 1935, Apr. 2012.

[7] M. Boban, T. T. V. Vinhoza, M. Ferreira, J. Barros, and O. K. Tonguz, "Impact of Vehicles as Obstacles in Vehicular Ad Hoc Networks," *IEEE Journal on Selected Areas in Communications*, vol. 29, no. 1, pp. 15–28, Jan. 2011.

[8] B. Yu and F. Bai, "ETP: Encounter Transfer Protocol for Opportunistic Vehicle Communication," in *Proc. of IEEE Infocom*, 2011.

[9] A. D. May, *Traffic Flow Fundamentals*. Prentice-Hall, 1990.

[10] M. Li, Z. Yang, and W. Lou, "Codeon: Cooperative Popular Content Distribution for Vehicular Networks using Symbol Level Network Coding," *IEEE Journal on Selected Areas in Communications*, vol. 29, no. 1, pp. 223–235, Jan. 2011.

[11] Q. Yan, M. Li, Z. Yang, W. Lou, and H. Zhai, "Throughput Analysis of Cooperative Mobile Content Distribution in Vehicular Network Using Symbol Level Network Coding," *IEEE Journal on Selected Areas in Communications*, vol. 30, no. 2, pp. 484–492, Feb. 2012.

[12] Y. Zhang and G. Cao, "V-PADA: Vehicle-Platoon Aware Data Access in VANETs," *IEEE Transactions on Vehicular Technology*, vol. 60, no. 5, pp. 2326 – 2339, June 2011.

[13] G. Yan and S. Olariu, "A Probabilistic Analysis of Link Duration in Vehicular Ad hoc Networks," *IEEE Transactions on Intelligent Transportation Systems*, vol. 12, no. 4, pp. 1227–1236, Dec. 2011.

[14] W. Zhang, Y. Chen, Y. Yang, X. Wang, Y. Zhang, X. Hong, and G. Mao, "Multi-Hop Connectivity Probability in Infrastructure-Based Vehicular Networks," *IEEE Journal on Selected Areas in Communications*, vol. 30, no. 4, pp. 740 –747, May 2012.

[15] Y. Zhuang, J. Pan, Y. Luo, and L. Cai, "Time and Location-Critical Emergency Message Dissemination for Vehicular Ad-Hoc Networks," *IEEE Journal on Selected Areas in Communications*, vol. 29, no. 1, pp. 187–196, Jan. 2011.

[16] F. Bai, D. D. Stancil, and H. Krishnan, "Toward Understanding Characteristics of Dedicated Short Range Communications (DSRC) from a Perspective of Vehicular Network Engineers," in *Proc. of ACM Mobicom*, 2010.

[17] S. Yousefi, E. Altman, R. El-Azouzi, and M. Fathy, "Analytical Model for Connectivity in Vehicular Ad Hoc Networks," *IEEE Transactions on Vehicular Technology*, vol. 57, no. 6, pp. 3341–3356, Nov. 2008.

[18] S. Ahn, M. J. Cassidy, and J. Laval, "Verification of a Simplified Car-Following Theory," *Transportation Research Part B: Methodological*, vol. 38, no. 5, pp. 431–440, 2004.

[19] D. R. Cox and H. D. Miller, *The Theory of Stochastic Processes*. Chapman & Hall/CRC, 1977.

[20] H. Hartenstein and K. Laberteaux, *VANET: Vehicular Applications and Inter-Networking Technologies*. Wiley, 2010.

[21] L. Cheng, B. E. Henty, D. D. Stancil, F. Bai, and P. Mudalige, "Mobile Vehicle-to-Vehicle Narrow-band Channel Measurement and Characterization of the 5.9 GHz Dedicated Short Range Communication (DSRC) Frequency Band," *IEEE Journal on Selected Areas in Communications*, vol. 25, no. 8, pp. 1501–1516, Oct. 2007.

[22] J. Yoo, B. S. C. Choi, and M. Gerla, "An Opportunistic Relay Protocol for Vehicular Road-side Access with Fading Channels," in *Proc. of IEEE ICNP*, 2010.

[23] F. Bai and B. Krishnamachari, "Spatio-Temporal Variations of Vehicle Traffic in VANETs: Facts and Implications," in *Proc. of ACM VANET*, 2009, pp. 43–52.

[24] J. J. Haas, Y. C. Hu, and K. P. Laberteaux, "Real-World VANET Security Protocol Performance," in *Proc. of IEEE Globecom*, 2009.

[25] Q. Chen, F. Schmidt-Eisenlohr, D. Jiang, M. Torrent-Moreno, L. Delgrossi, and H. Hartenstein, "Overhaul of IEEE 802.11 Modeling and Simulation in NS-2," in *Proc. of ACM MSWiM*, 2007.

[26] D. Jiang, Q. Chen, and L. Delgrossi, "Optimal Data Rate Selection for Vehicle Safety Communications," in *Proc. of ACM VANET*, 2008.